Int. J. Multiphase Flow Vol. 19, No. 1, pp. 51–63, 1993
Printed in Great Britain

0301-9322/93 $6.00 + 0.00
Pergamon Press Ltd

THERMO-HYDRAULICS OF BOILING TWO-PHASE FLOW IN HIGH CONVERSION LIGHT WATER REACTORS (THERMO-HYDRAULICS AT LOW VELOCITIES)

M. ARITOMI, T. MIYATA, M. HORIGUCHI and A. SUDI
Research Laboratory for Nuclear Reactors, Tokyo Institute of Technology, 2-12-1 Ohokayama, Meguro-ku, Tokyo 152, Japan

(Received 11 June 1991; in revised form 25 May 1992)

Abstract—With the aim of obtaining a fundamental data base with regard to HCLWR (high conversion light water reactor) core thermo-hydraulics, the effect of channel gaps on thermo-hydraulic behavior is investigated, particularly at low velocities as these may be assumed to occur under various abnormal operating conditions in HCLWRs. Boiling heat transfer and frictional loss are investigated experimentally, and the applicability of the drift flux model to narrow channels is examined. Finally, the reflooding behavior is investigated experimentally in relation to a postulated loss-of-coolant accident in HCLWRs. It has been made clear from the results that the incidence of a pressure drop during the reflooding phase is much higher than that in current LWRs.

Key Words: boiling two-phase flow, high conversion light water reactor, thermo-hydraulics

1. INTRODUCTION

One of the fundamental policies of the nuclear industry in Japan is to reprocess spent fuel generated from existing light water reactors (LWRs) in order to reuse the recovered plutonium. There are plans to construct a reprocessing plant, whose process capability is 800 ton/year, on Shimokita Peninsula. Furthermore, plutonium recovered by reprocessing in overseas facilities will return to Japan at a later date. The Japanese nuclear policy that spent fuel generated from LWRs should be reprocessed was adopted on the condition that fast breeder reactors (LMFBRs) would be developed along with the reprocessing of fuel. However, the development of LMFBRs has slowed down throughout the world for both economic and public reasons. In Japan, it is said that LMFBRs will be introduced as commercial reactors after 2030 onward, and the next generation of LWRs may be the major nuclear power source in the early 21st century. One of the most important problems facing the Japanese nuclear policy is, therefore, how effectively plutonium should be used. Although it is assumed as a matter of urgency that plutonium will be burnt in LWRs, the mixed-oxide fuel (MOX) is much more expensive than that using enriched uranium. As the burn-up increases in current LWRs, ^{242}Pu accumulates so the quality of the plutonium decreases. Consequently, it is difficult to use the plutonium reprocessed from MOX spent fuel as the fuel for LMFBRs. Another question which arises regarding the reprocessing is how transuranic elements are annihilated.

The concept of a high conversion LWR (HCLWR) was proposed by Edlund (1975) and Oldekop *et al.* (1982). The original aim of the HCLWR was to enhance the utilization rate of uranium by increasing the conversion ratio. However, it is more attractive for the HCLWR to be able to maintain the quality of the plutonium even for high burn-up, and to have the possibility of annihilating transuranic elements due to the reasonance absorption. To harden the neutron spectrum, the volumetric ratio of moderator to fuel is decreased to 1, though the ratio in current LWRs is about 2. For this purpose, a high density hexagonal lattice core will be adopted. Therefore, it becomes important to understand the core-heat removal characteristics, both in normal and abnormal operating conditions, resulting from a lower water inventory in the core and the use of narrow coolant channels. However, our present knowledge of such core-heat removal characteristics is too limited to apply them to the thermal and safety designs of the HCLWR.

The purpose of this study is to obtain the necessary fundamental data base for deciding the development target of the next generation of LWRs in the next few years in Japan, i.e. to clarify

the difference in the thermo-hydraulic behavior in narrower channels from that in current LWRs and to take out the subjects required for proof tests. In our previous paper (Inoue *et al.* 1988), boiling heat transfer, critical heat flux and pressure drop were investigated experimentally for normal operating conditions using Freon 113 as the test fluid. In this paper, the effect of the channel gap on the thermo-hydraulic behavior is investigated at low velocities which may appear under various abnormal operating conditions in HCLWRs. At first, boiling heat transfer and frictional loss are investigated experimentally. Next, based on these results, the applicability of the drift flux model (used for the two-phase flow analysis in current LWRs) is examined. Finally, the reflooding behavior in narrow channels, which may appear during a postulated loss-of-coolant accident, is investigated experimentally.

2. EXPERIMENTAL APPARATUS

Figure 1 illustrates a schematic diagram of the loop operated at atmospheric pressure. Freon 113 was used as the test fluid. The loop was devised to suppress the flow circulation pump-induced fluctuation by the adoption of sufficient head and adequate throttling in the upstream to the test section. The vapor generated in the test section was separated in a separator and was liquified in a condenser connected to the separator. A preheater and a precooler were equipped to maintain the liquid temperature at the entrance of the test section at the required value. The other function of the precooler was to protect the circulation pump from cavitation. A bypass line was installed parallel to the test section to facilitate the initial condition for the reflooding tests. The flow rate of Freon 113 was regulated by a flow control valve and was measured by an orifice flowmeter.

Two test sections were prepared in this work. The geometry and dimensions of test section A are presented in Figure 2. The inner rod was a heater rod made of a sheath heater (10 mm o.d.

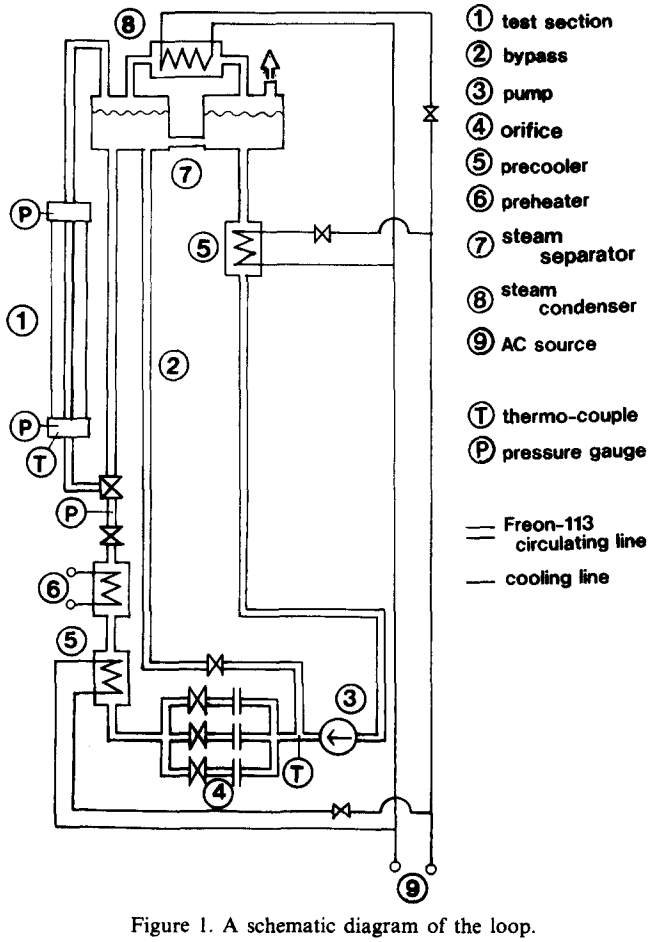

Figure 1. A schematic diagram of the loop.

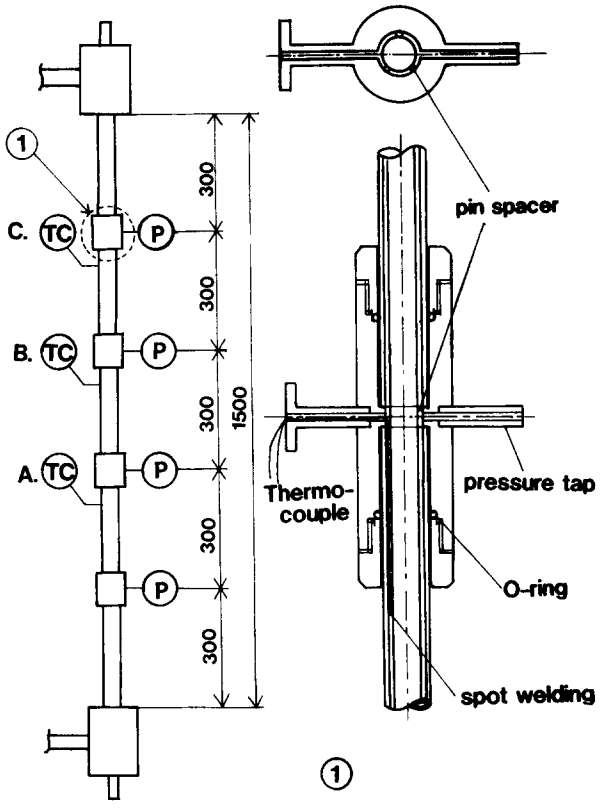

Figure 2. Test section A.

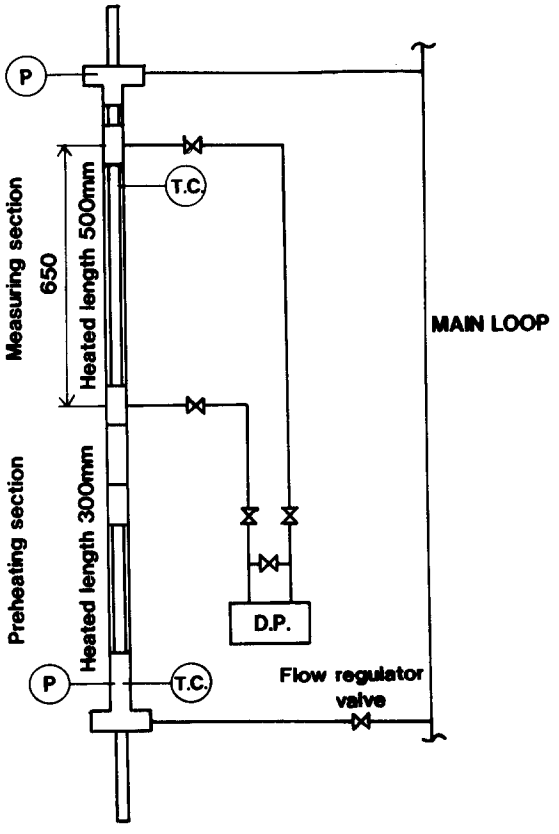

Figure 3. Test section B.

Table 1. Experimental conditions

Test fluid	Freon 113
System pressure	Atmospheric pressure
Inlet velocity	0.02–0.4 m/s
Inlet temperature	35–45°C
Heat flux	0–100 kW/m²
Channel gap	0.5, 1.0, 2.0 mm
Initial wall temperature (reflooding test only)	150–300°C

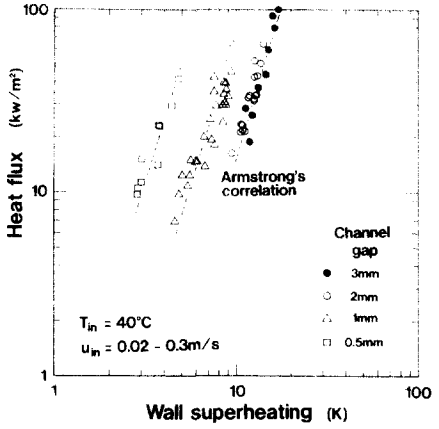

Figure 4. Effects of the channel gap on saturated nucleate boiling heat transfer.

and 1000 mm long), on the surface of which enamelled chromel and alumel wires (0.1 mm o.d.) were separately welded on as close as possible to measure the heated wall temperature. The thermocouples were attached at several points along the channels. The channel gap was varied by changing the inner diameter of the outer tube, consisting of five Pyrex glass tubes and four connectors. Pressure taps and thermocouple drawers were also included together with stainless steel connectors. Figure 3 shows the other test section B, used especially for the annular mist flow experiments. It was divided into two sections to attain stable annular flow conditions: one was a 300 mm long preheated section to establish stable annular mist flow conditions; the other was a 500 mm long measurement section individually heated. The designs of both sections were the same as test section A. The experimental conditions are listed in table 1.

Test sections A and B were used for steady-state tests where the inlet fluid temperature, flow rate and heat flux were controlled. Test section A was also used for the reflooding tests. While Freon 113 was flowing at a regulated temperature and velocity through the bypass, the heater rod was heated up to the desired temperature. When these conditions were established, the bypass was closed and the fluid flowed into the test section. The changes in the wall temperature and pressure drop between the inlet and exit of the heated section were measured continuously with time. The quenching velocity was obtained from the time difference in the abrupt change in wall temperatures detected at two different measuring points. Although the outer tube surface was superheated while the fluid was flowing through the bypass, a liquid film formed on its surface immediately after the fluid was injected. Therefore, the outer tube surface condition was saturated during measurements.

3. THERMO-HYDRAULICS AT STEADY STATE

3.1. Heat transfer

The effect of the flow channel gap on nucleate boiling heat transfer was investigated experimentally. The boiling curves are shown in Fig. 4. The results indicated that, so far as the experimental conditions tested in this study are concerned, saturated nucleate boiling heat transfer in a narrow channel is independent of the inlet velocities—just like the heat transfer behavior in normal channels such as the wider coolant flow channels in current LWRs. In figure 4, the results obtained in our previous study for a 3 mm channel gap (Aritomi *et al.* 1986) are included. It is noted that saturated nucleate boiling heat transfer for gaps >2 mm is not influenced by the gap size. Our previous study (Aritomi *et al.* 1986) revealed that saturated boiling heat transfer with Freon 113 at atmospheric pressure was in agreement with Armstrong's (1966) correlation; Armstrong's correlation is illustrated by the solid line in figure 4. The experimental results for gaps of 2 and 3 mm correlate well with this.

Saturated nucleate boiling heat transfer in channel gaps of 0.5 and 1 mm increases with a decrease in the channel gap. The number of bubbles departing from the heated wall increases in inverse proportion to the cross section of the channel. Consequently, the turbulence induced by bubble

departure is enhanced. Furthermore, the microlayer underneath a growing bubble becomes thinner with a decrease in the channel gap, because the bubble is distorted and flattened due to the existence of the outer tube (Aoki *et al.* 1982). These effects are thought to be the reason for the enhancement of nucleate boiling heat transfer when the channel gap is reduced. If the former effect were more dominant for channel gaps >2 mm, boiling heat transfer would be enhanced for narrower channels. This is, however, contradictory to our observation in figure 4. It is therefore supposed that the latter effect is more dominant for enhancing boiling heat transfer in narrowing channels.

For channel gaps of 0.5 and 1 mm, the slope of the boiling curve agrees with the trend of Armstrong's (1966) correlation. Based on our experimental data of 0.5, 1.0 and 2.0 mm, the following empirical correlations, which are shown also in figure 4, are obtained:

$$\Delta T_{sat} = 0.157\,\delta^{*0.75} q''^{0.293} \quad (22.2 \leqslant \delta^* \leqslant 88.7), \qquad [1]$$

where δ^* is a dimensionless channel gap defined by

$$\delta^* = \frac{\delta}{\left(\frac{\nu_L^2}{g}\right)^{1/3}}, \qquad [2]$$

q'' is the heat flux and ΔT_{sat} is the wall superheating. Armstrong's (1966) correlation is applicable for channel gaps >2.0 mm:

$$\Delta T_{sat} = 4.55 q''^{0.293} \quad (88.7 \leqslant \delta^*). \qquad [3]$$

Next, the heat transfer characteristics in annular mist flow under low velocity and low heat flux conditions, which may appear under various transient conditions in the HCLWR core, were investigated. Heat transfer in annular mist flow has been reported elsewhere by many researchers (Bennett *et al.* 1961; Collier *et al.* 1964; Dengler & Addoms 1956; Schrock & Grossman 1959). Heat transfer with dominant liquid film evaporation has also been studied to a considerable degree. It is clear from previous works that the heat transfer coefficient under this condition is well-correlated in terms of the Lockhart–Martinelli parameter. Hence, we attempted to relate our experimental results to several proposed correlations. The experimental data for a 2 mm channel gap is compared in figure 5 with the correlation of Collier *et al.* (1964), which was obtained from experiments with water. It is quite reasonable to think that the empirical constant in their correlation may be different from the trend in our experimental results with Freon 113, whereas the dimensionless heat transfer coefficient can be correlated in terms of the Lockhart–Martinelli parameter, as shown in the figure.

In fact, as shown in figure 6, Collier's method does not correlate well with the data for a channel gap of 0.5 mm. Figures 5 and 6 indicate that the general trend in heat transfer for channel gaps >2 mm is in agreement with that in normal channels, i.e. it follows Collier's correlation except for the proportionality constant. However, for channel gaps <1 mm it is different from that in normal channels.

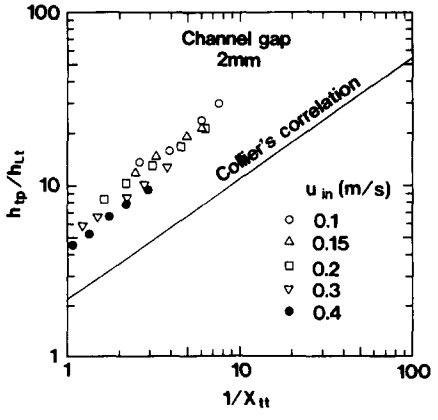

Figure 5. Comparison of Collier *et al.*'s (1964) correlation with the experimental results for a 2 mm channel gap.

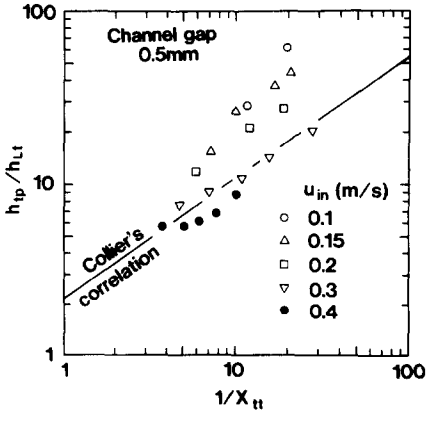

Figure 6. Comparison of Collier *et al.*'s (1964) correlation with the experimental results for a 0.5 mm channel gap.

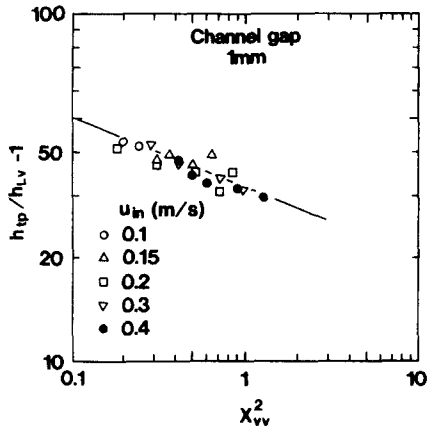

Figure 7. Plot of the vaporization heat transfer of the liquid film in annular mist flow based on a laminar flow model.

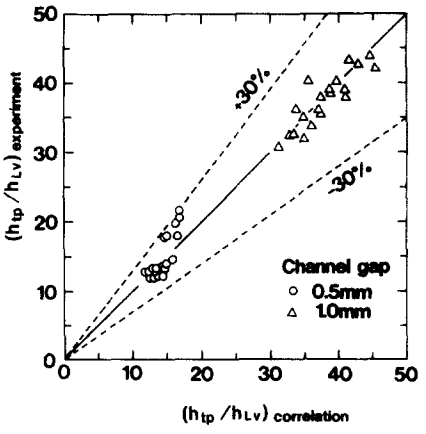

Figure 8. Comparison of the proposed correlation with the experiments.

Since the experimental data indicated that the heat transfer in channel gaps < 1 mm is independent of the inlet velocity, the results are plotted against the Lockhart–Martinelli parameter (χ) based on a laminar flow model. Typical results are shown in figure 7. This plot correlates well with the data. Thus, the effect of the channel gap on heat transfer is expressed by the following empirical correlations:

$$\frac{h_{tp}}{h_{Lt}} = 5.5\frac{1}{\chi_{tt}^{0.7}} \quad (88.7 \leqslant \delta^*) \qquad [4]$$

and

$$\frac{h_{tp}}{h_{Lv}} = 1 + 0.0172\,\delta^{*1.67}\frac{1}{\chi_{vv}^{0.4}} \quad (22.2 \leqslant \delta^* \leqslant 44.4); \qquad [5]$$

where h is the heat transfer coefficient and the subscripts tp, Lt, tt, Lv and vv indicate two-phase flow, liquid turbulent flow, turbulent flow, liquid turbulent flow and laminar flow, respectively. A comparison of [4] with the experiments is shown in figure 8.

Since the liquid film flow on the heated surface fluctuated considerably at low velocities in near-critical heat fluxes, satisfactory reproducibility of the dryout heat flux data has not been obtained in this work.

3.2. Pressure drop

The pressure drop of boiling two-phase flow was measured in two kinds of test section to clarify whether or not the existing correlations of friction loss and the drift flux model used for normal flow channels are applicable for narrow channels. In test section A, the pressure drops were measured over two different distances (i.e. the pressure drop between two locations near the exit of the heated section where the flow has already become saturated, and the other between the inlet and outlet pressure taps located in the heated section) to establish an evaluation method of pressure drop for the whole flow regime, including subcooled boiling two-phase flow. Test section B was used for measuring the pressure drop in annular mist flow. The experimental results in saturated boiling two-phase flow were analyzed numerically using a drift flux model incorporating the following conventional distribution parameter (C_0) and drift velocity (V_{gj}):

$$\begin{aligned} C_0 &= \left[1.2 - 0.2\left(\frac{\rho_G}{\rho_L}\right)^{0.5}\right][1 - \exp(-18\epsilon)] && (0 \leqslant \epsilon \leqslant 0.6) \\ &= 50\epsilon^3 - 105\epsilon^2 + 72\epsilon - 15 && (0.6 < \epsilon \leqslant 0.8) \\ &= 1 && (0.8 < \epsilon) \end{aligned} \qquad [6]$$

and

$$V_{gj} = 1.414\left[\frac{\sigma g(\rho_L - \rho_G)}{\rho_L^2}\right]^{0.25}, \qquad [7]$$

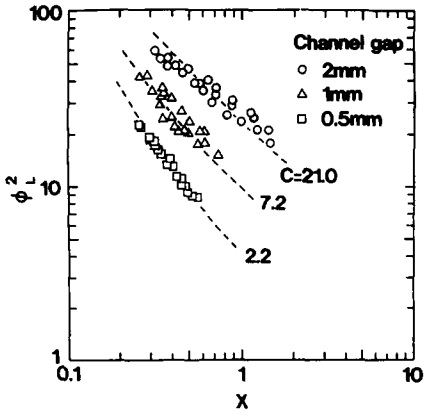

Figure 9. Effects of the channel gap on the two-phase friction multiplier.

where ϵ is the void fraction, ρ is the density, σ is the surface tension and the subscripts G and L indicate gas and liquid, respectively. In general, the drift velocity greatly influences the bubbly flow characteristics. However, it scarcely influences the flow characteristics in annular mist flow because the phasic volumetric velocity is much higher than the drift velocity. Therefore, only one representative correlation was used commonly for all flow regimes. It is noted here that in our experiments the slug flow regime was not observed for channel gaps <2 mm and a sudden transition from bubbly flow to churn turbulent flow took place with an increase in quality (x).

In the numerical analysis, the void fraction at each node along the channel was calculated by [8] using interpolation of the measured pressure by polynominal approximation:

$$\frac{1}{\epsilon} = C_0\left(1 + \frac{1-x}{x}\frac{\rho_G}{\rho_L}\right) + \frac{V_{gj}}{x\rho_G}. \qquad [8]$$

The acceleration and hydrostatic losses were calculated by integrating a momentum conservation equation of the mixture and the friction loss was obtained by

$$\Delta P_{fric} = \Delta P_{meas} - \Delta P_{acc} - \Delta P_{head}, \qquad [9]$$

where ΔP_{fric} is the friction loss, ΔP_{meas} is the measured pressure drop, ΔP_{acc} is the acceleration loss and ΔP_{head} is the hydrostatic loss.

The friction loss thus calculated was plotted as the two-phase friction multiplier (ϕ_L^2) vs the Lockhart–Martinelli parameter (χ) in figure 9 for saturated boiling conditions. Using Chisholm's (1967) correlation:

$$\phi_L^2 = 1 + \frac{C}{\chi} + \frac{1}{\chi^2} \qquad [10a]$$

and

$$\chi = \chi_{tt} \quad \text{for } Re_L \geqslant 2300$$
$$= \chi_{vv} \quad \text{for } Re_L < 2300, \qquad [10b]$$

where Re_L is the Reynolds number in the liquid phase. The constant C is determined by least-squares fitting as demonstrated in figure 9 by the solid lines. Chisholm (1967) recommended C = 21 for normal flow channels. This value agrees with the present experiments for a 2 mm channel gap. Since the flow is considered to be almost laminar under the present experimental conditions for gaps of 0.5 and 1 mm, the value of C decreases as the channel becomes narrower. On the basis of these results, the following empirical correlation for C is proposed:

$$C = 0.0161\,\delta^{*1.6} \quad (22.2 \leqslant \delta^* \leqslant 88.7). \qquad [11]$$

The broken lines in figure 9 represent [11]. With the help of [11], the pressure drops in test section A were analyzed numerically based on a drift flux model. In the numerical analysis, for the assumed inlet pressure in the heated section, the mass, energy and momentum conservation equations were

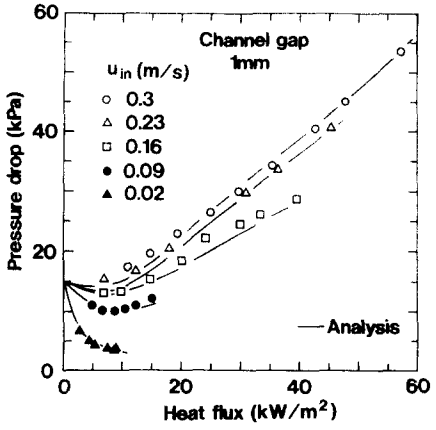

Figure 10. Comparison of the drift flux model with the experiments with a 1 mm channel gap.

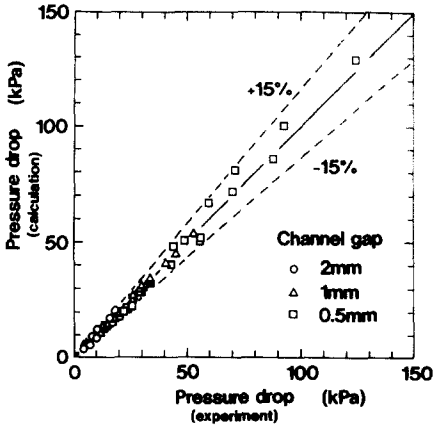

Figure 11. Comparison of the drift flux model for various channel gaps with experimental pressure drops.

solved by the Runge–Kutta–Gill method. If the calculated exit pressure in the heated section did not agree with the measured pressure, iterative computations were performed by changing the inlet pressure. Pressure drops in the heated section were thus obtained. The true quality in the subcooled boiling region was evaluated by the model proposed in our previous paper (Inoue *et al.* 1988).

Typical results showing a comparison of the present numerical analysis with experiments are given in figure 10. Figure 11 also demonstrates a comparison between the calculation and the measurements covering all the flow regimes from subcooled boiling to annular mist flow. It can be seen from figures 10 and 11 that the drift flux model in conjunction with [11] is also applicable for evaluating the pressure drop in all the regimes from subcooled boiling to annular mist flow in narrow channels.

4. REFLOODING BEHAVIOR

It is most important from the viewpoint of reactor safety to clarify whether or not the emergency core cooling systems adopted in current LWRs are applicable for HCLWRs with a high density

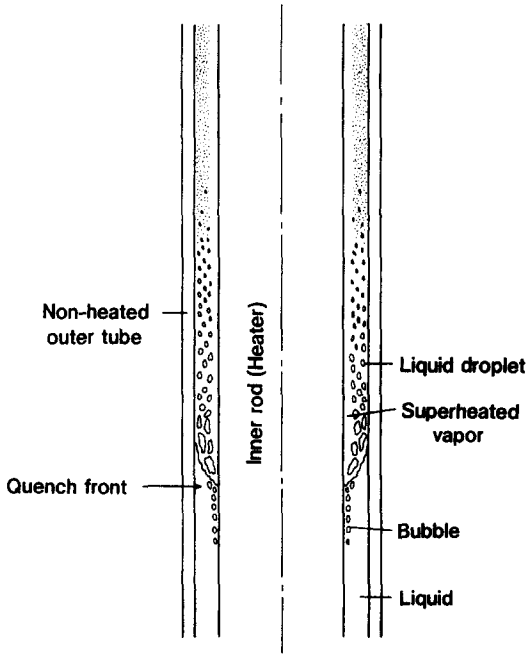

Figure 12. Sketch of the flow characteristics during a reflooding phase.

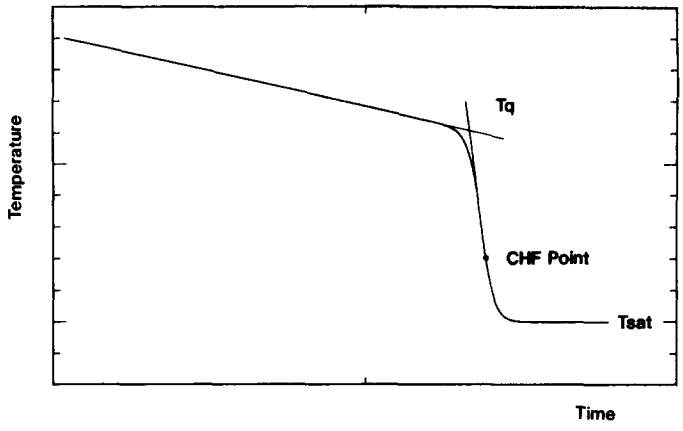

Figure 13. Sketch of the wall temperature history during a reflooding phase.

hexagonal lattice core. In this vein, the reflooding behavior was investigated experimentally using narrow channels to understand the bottom quenching during a reflooding phase in an HCLWR.

The velocity of the vapor generated by boiling is so high at a quench front that the reflooding liquid is dispersed into vapor flow as a number of small droplets, as shown in figure 12, since we used the test section with a channel gap <2 mm. Downstream of the quench front, both inverted annular flow and inverted churn turbulent flow, which are encountered during a reflooding phase in normal channels, are not observed in the present case. This is because the thin liquid film flows only on the non-heated outer tube, and the superheated vapor entraining many small liquid droplets flows in the core of the flow passage. A typical wall temperature history is illustrated in figure 13. The quenching temperature is determined here in the same manner as usually done in much of the literatures.

Typical results showing the effects of the initial wall temperature and reflooding velocity (u_{in}) on the quench velocity are shown in figure 14. Although the quench velocity is the same order of magnitude as the reflooding velocity in normal channels, it is much lower than the reflooding velocity in the present narrow channels. This behavior is very similar to the top quenching behavior caused by a falling liquid film (Abe *et al.* 1986).

In view of the very small quenching velocity observed in the present narrow channels, we interpret the present results as follows. The quenching is closely related to the heat transfer characteristics in the downstream near the quench front. The vaporization rate at the quench front is dependent on the wall temperature. As the vapor velocity increases, the ratio of the dispersed liquid rate to the reflooding rate increases and the liquid holdup decreases. In general, the heat transfer from the heated surface to the fluid is much lower in superheated dispersed flow than those in inverted annular flow and inverted churn turbulent flow. On the other hand, the vaporization rate is not strongly dependent on the reflooding velocity and channel gaps. Therefore, even though the channel gap becomes wider and the reflooding velocity higher, the vaporization rate scarcely

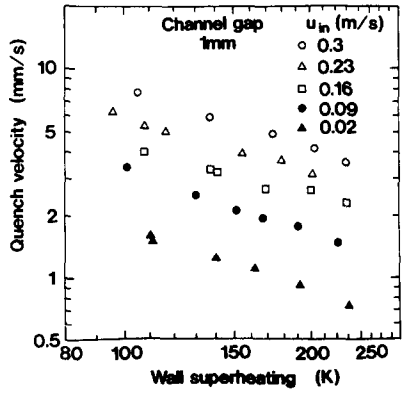

Figure 14. Effects of wall superheating on the quench velocity.

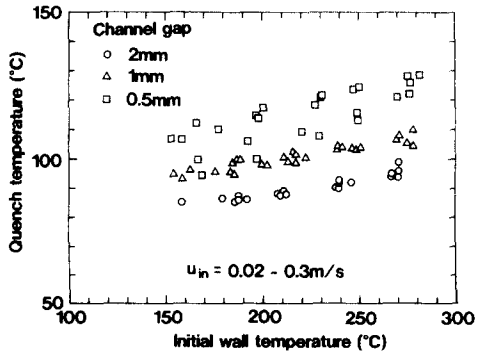

Figure 15. Effects of the initial wall temperature and channel gap on the quench temperature.

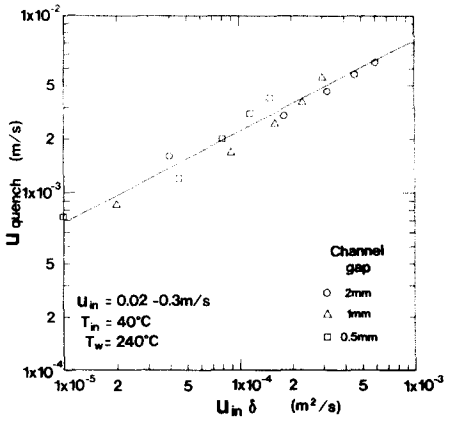

Figure 16. Relationship between quench velocity and the product of the reflooding velocity and channel gap.

changes and the liquid holdup in the downstream close to the quench front increases. Consequently, the quench velocity decreases with an increase in the initial wall temperature and with decreases in the channel gaps and reflooding velocity.

Figure 15 shows the relationship between the initial wall temperature and the quench temperature, including the data at various reflooding velocities. The quench temperature is shown to be almost independent of the reflooding velocity. Moreover, the initial wall temperature does not greatly influence the quench temperature. As the flow channel gap becomes narrower, the quench temperature increases. Since the vapor velocity is inversely proportional to the flow area, the ratio of the liquid rate contributing to quenching to the dispersed liquid rate decreases with an increase in the vapor velocity.

Next, the effect of the reflooding velocity and flow channel gap on the quench velocity will be mentioned. Figure 16 shows the relationship between the quench velocity and the product of the reflooding velocity and flow channel gap. It is seen in figure 16 that the quench velocity is in proportion to the square root of the product.

By considering the results shown in figures 14 and 16, the following dimensionless parameters are introduced to present the reflooding velocity and wall superheating:

$$\mathrm{Re}_{\mathrm{in}} = \frac{u_{\mathrm{in}}(2\delta)}{\nu_{\mathrm{L}}} \qquad [12]$$

and

$$\Delta T^{*}_{\mathrm{sat}} = \frac{Cp_{\mathrm{G}}\,\Delta T_{\mathrm{sat}}}{L}. \qquad [13]$$

Next, considering that the vapor and liquid densities and surface tension dominate the quenching velocity, the following parameter, which influences the heat transfer coefficient in inverted annular flow (Aritomi & Inoue 1988), is also introduced:

$$d^{*} = \left[\frac{\sigma}{(\rho_{\mathrm{L}} - \rho_{\mathrm{G}})g}\right]^{0.5}. \qquad [14]$$

All experimental results are arranged in terms of these parameters. The following empirical correlation is obtained:

$$\mathrm{Re}_{\mathrm{quench}} = 0.059\,\mathrm{Re}_{\mathrm{in}}^{0.5}\,\Delta T^{*-1}_{\mathrm{sat}}, \qquad [15]$$

where

$$\mathrm{Re}_{\mathrm{quench}} = \frac{u_{\mathrm{quench}} d^{*}}{\nu_{\mathrm{L}}}. \qquad [16]$$

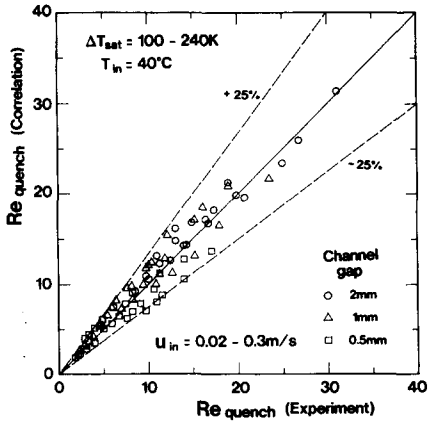

Figure 17. Comparisons of the proposed correlation with the measured quench velocity.

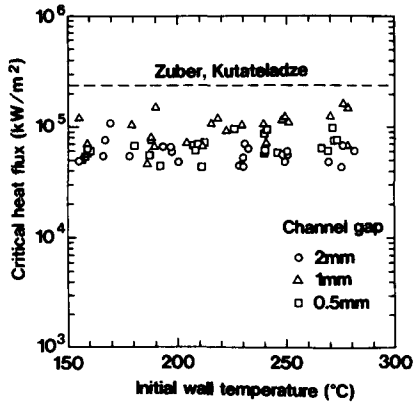

Figure 18. Effects of the initial wall temperature and channel gap on the critical heat flux.

Comparisons of the proposed correlation, [15], with the experimental results are shown in figure 17. Equation [15] correlates well with the experimental results for channel gaps of 0.5–2 mm and at inlet velocities of 0.02–0.3 m/s. Based on the heated wall temperature histories, the transient two-dimensional thermal conduction equation was solved numerically in the heater to obtain the time-varying heat flux. Thus, the calculated maximum heat fluxes appearing after quenching are demonstrated in figure 18, showing no clear dependences on the flow channel gap, reflooding velocity and initial wall temperature. The longitudinal heat conduction is significantly large because of the 1 mm wall thickness. The quenching characteristics are governed by the thermal properties of the heated wall, i.e. density, specific heat and thermal conductivity. Since these properties are constant in the present test section, the wall superheating at maximum heat flux is almost equal under various conditions.

Typical results of the maximum pressure drop in heated sections during the reflooding phase are shown in figure 19. The effect of the channel gap on the maximum pressure drop is given in figure 20. Although it is difficult to discuss this effect quantitatively because of the scattered data points, the ratio of the maximum pressure drop between channel gaps of 0.5 and 1 mm almost agrees with that between channel gaps of 1 and 2 mm; i.e. the maximum pressure drop is inversely proportional to the channel gap. The maximum pressure drop is mainly due to the acceleration and friction losses in superheated mist flow. The vaporization rate at quenched front increases as the quench temperature becomes higher. It seems that the dispersed liquid (only a small contributor to quenching) increses as the vapor velocity at the quench front becomes higher.

If the core of the HCLWR was not covered by coolant during a postulated loss-of-coolant accident and coolant were to be injected into the reactor core, due to the difference in the hydrostatic head between the downcomer and the reactor core, the pressure drop might be too great

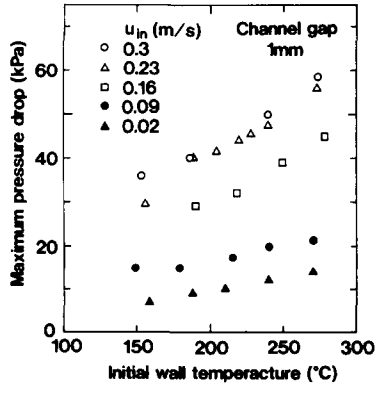

Figure 19. Maximum pressure drop during a reflooding phase for a 1 mm channel gap.

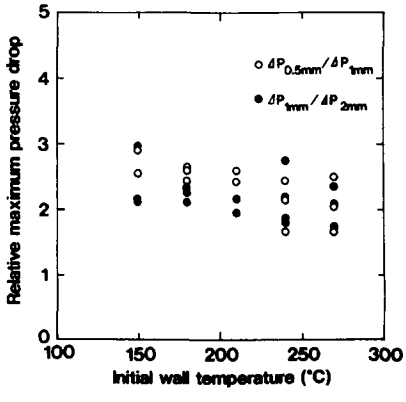

Figure 20. Relative maximum pressure drop for different channel gaps.

to have a sufficiently high reflooding velocity to prevent clads from being heated excessively. Hence, it is definitely necessary for the safety design of HCLWRs to ensure that the core remains covered by coolant during any transient or accident phase.

5. CONCLUSIONS

The thermo-hydraulic behavior of boiling two-phase at low velocity, which may appear under various abnormal operating conditions in an HCLWR, was investigated in narrow channels. The reflooding behavior simulating bottom quenching in an HCLWR core accident was also studied experimentally. The following points have been clarified:

(1) Boiling heat transfer and the pressure drop in channel gaps >2 mm can be evaluated in the same way as those in normal channels, but those in channel gaps <2 mm cannot be evaluated by the same correlations.
(2) Saturated nucleate boiling heat transfer in channel gaps <2 mm is influenced by the gap spacing. An empirical correlation for the heat transfer, [2], is proposed.
(3) Heat transfer in annular mist flow in channel gaps <1 mm depends on the channel gap as well as the Lockhart–Martinelli parameter. An empirical correlation for the heat transfer, [5], is proposed.
(4) The two-phase friction multiplier is dependent on the channel gap in the range below 2 mm, whereby an empirical correlation, [11], is proposed.
(5) The drift flux model which is usually applied for normal channels is also applicable for boiling two-phase flow with a channel gap <2 mm, as long as the correlation of the two-phase flow friction multiplier, [11], which considers the effects of the gap size, is constituted in the model.
(6) In channel gaps <2 mm, the reflooding liquid is immediately dispersed into the vapor as a number of small droplets at the quench front, since the vapor velocity generated due to boiling at the quench front is very high. Consequently, neither inverted annular flow nor inverted churn turbulent flow appear downstream of the quench front. Superheated mist flow occurs. Hence, the ratio of the liquid rate contributing to quenching to the reflooding rate is very small and the quench velocity is much lower than the reflooding velocity. The quench velocity is in proportion to the square root of the product of the reflooding velocity and the channel gap, and is inversely proportional to the wall superheating. An empirical correlation, [16], is proposed.
(7) The pressure drop in the narrow channel is very high during the reflooding phase because of the high velocity superheated mist flow.

These conclusions are drawn on the basis of the experimental results using only Freon 113. Further investigation using other fluids is necessary to generalize these conclusions.

REFERENCES

ABE, Y., SOBAJIMA, M. & MURAO, T. 1986 Experimental study of effects of upward stream flow rate on quench propagation by falling water film. *J. Nucl. Sci. Technol.* **23,** 415–432.

AOKI, S., ARITOMI, M. & SAKAMOTO, Y. 1982 Experimental study on the boiling phenomena within a narrow gap. *Int. J. Heat Mass Transfer* **25,** 985–990.

ARITOMI, M. & INOUE, A. 1988 Thermo-hydraulic behavior of inverted annular flow, effects of flow direction and channel diameter. In *Proc. Japan–U.S. Semin. on Two-phase Flow Dynamics*, Japan, pp. J.3.1–J.3.8.

ARITOMI, M., AOKI, S. & INOUE, A. 1986 Thermo-hydraulic instabilities in parallel boiling channel systems, Part 2. Experimental results. *Nucl. Engng Des.* **95,** 117–127.

ARMSTRONG, R. J. 1966 The temperature difference in nucleate boiling. *Int. J. Heat Mass Transfer* **9,** 1148–1149.

BENNETT, J. A. R., COLLIER, J. G., PRATT, H. R. C. & THORNTON, J. D. 1961 Heat transfer to two-phase gas–liquid systems, Part I. Steam/water mixtures in the liquid dispersed region in an annulus. *Trans. Instn. Chem. Engrs* **39,** 113–126.

CHISHOLM, D. 1967 Pressure gradients during the flow of an incompressible two-phase mixture through pipes, venturis and orifice plates. *Br. Chem. Engng* **12,** 454–457.

COLLIER, J. G., LACEY, P. M. C. & PULLING, D. J. 1964 Heat transfer to two-phase gas–liquid systems, Part II. Further data on steam/water mixtures in the liquid dispersed region in an annulas. *Trans. Instn Chem. Engrs* **43,** 127–139.

DENGLER, C. E. & ADDOMS, J. N. 1956 Heat transfer mechanism for vaporization of water in a vertical tube. *Chem. Engng Prog. Symp. Ser.* **52,** 95–103.

EDLUND, M. C. 1975 High conversion ratio plutonium recycle in pressurized water reactors. *Ann. Nucl. Energy* **2,** 801–807.

INOUE, A., ARITOMI, M. & JINBO, M. 1988 Fundamental study on boiling two-phase flow and critical heat flux in a narrow heated channel with a wire spacer. In *Proc. 3rd Int. Top. Mtg on Nuclear Power Plant Thermal Hydraulics and Operations*, Seoul, S. Korea, Vol. 1, pp. A2.77–A2.84.

OLDEKOP, W., BERGER, H. D. & ZEGGEL, W. 1982 General features of advanced pressurized water reactors with improved fuel utilization. *Nucl. Technol.* **59,** 212–227.

SCHROCK, V. E. & GROSSMAN, L. M. 1959 Forced convection boiling studies. Forced convection vaporization project. Report TID-14639.